RSC Advances

ROYAL SOCIETY OF CHEMISTRY

www.rsc.org/advances

Cite this: DOI: 10.1039/c0xx00000x

www.rsc.org/xxxxxx

COMMUNICATION

Donor atom selective coordination of Fe^{3+} and Cr^{3+} trigger fluorophore specific emission in a rhodamine-naphthalimide dyad

Narendra Reddy Chereddy,*[a,b] Krishnan Saranraj,[a] Ayan Kumar Barui,[c] Chitta Ranjan Patra*[c], Vaidya Jayathirtha Rao*[b] and Sathiah Thennarasu*[a]

Received (in XXX, XXX) Xth XXXXXXXXX 20XX, Accepted Xth XXXXXXXXX 20XX
DOI: 10.1039/b000000x

A rhodamine-naphthalimide dyad with multiple coordination sites displays Fe^{3+} and Cr^{3+} specific absorption and fluorescence emission profiles and permits specific detection of Fe^{3+} and Cr^{3+} ions present in aqueous samples, and live A549 and CHO cells in a chemoselective manner.

Iron and chromium are among the indispensable transition metal ions found in both humans and animals.[1-3] While Fe^{3+} acts as oxygen carrier in hemoglobin, and plays an important role in cellular metabolism and enzyme catalysis,[1] Cr^{3+} plays a critical role in several metabolic processes[2]. Accordingly, the deficiency as well as overload of Fe^{3+} has resulted in various biological disorders.[3] Similarly, deficiency of Cr^{3+} has lead to diabetes and cardiovascular diseases while excess of Cr^{3+} is carcinogenic and adversely affects cellular structures.[2] Consequently, several luminescent probes based on fluorescence 'turn-off' strategy have been developed for selective quantitative detection of Fe^{3+} or Cr^{3+} ions.[4-5] Recently, much effort has been devoted to develop fluorescence 'turn-on' probes for the selective detection of Fe^{3+} or Cr^{3+} ions,[6-7] overcoming the paramagnetic quenching nature of these ions. However, multianalyte sensing using single molecular probe is highly desirable as the environmental and biological samples usually contain a variety of ions. The multianalyte probes reported for the detection of both Fe^{3+} and Cr^{3+} ions, suffer from the cross sensitivity to Al^{3+} ions.[8] Moreover, these probes have a single binding site for both Fe^{3+} and Cr^{3+} ions, and display metal ion specific fluorescence emission in the same wavelength range. This drawback limits the application of these multianalyte probes in the real-time detection of Fe^{3+} and Cr^{3+} ions in biological samples. However, specific detection of Fe^{3+} and Cr^{3+} ions in living systems requires a multianalyte probe capable of displaying fluorescence response at different wavelengths. Although there are reports on multianalyte probes, varying conditions are applied to detect different analytes. To our knowledge, there is no report on a single molecular probe that emits fluorescence at two different wavelengths upon interaction with Fe^{3+} and Cr^{3+} ions, respectively. Consequently, development of new probes that can potentially sense both Fe^{3+} and Cr^{3+} ions in aqueous and biological systems with different fluorescence outputs, preferably with 'turn-on' emission is imperative for proper diagnosis and sensor applications.

In the present communication, we report a rhodamine-naphthalimide dyad **1** that senses Fe^{3+} and Cr^{3+} ions and emits

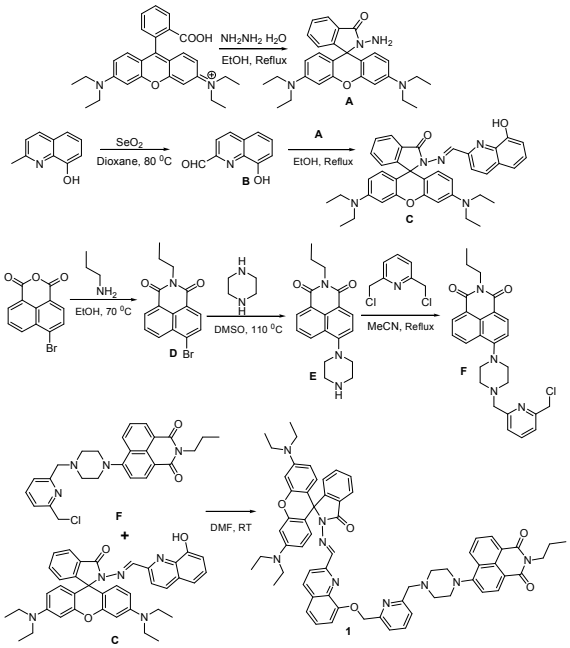

Scheme 1. Synthesis of rhodamine-naphthalimide dyad **1**

fluorescence at two different wavelengths. Non-interference of common metal ions, including Al^{3+}, found in biological samples is confirmed. A possible application of this single molecular probe for sensing Fe^{3+} and Cr^{3+} ions in cancerous A549 and non-cancerous CHO cells is demonstrated.

A new rhodamine-naphthalimide dyad **1** with multiple coordination sites for metal ion binding was synthesized as shown in **Scheme 1** and thoroughly characterized using NMR and ESI-HRMS analytical techniques (Figs. S1-S3, ESI†). The dyad probe **1** encompasses six potential donor atoms for metal ion chelation. Metal ion sensing properties of **1** were assessed using UV-visible and fluorescence techniques in aqueous acetonitrile (1:1 v/v 0.01 M Tris HCl-CH_3CN, pH 7.4) medium. The absorption spectrum of **1** (10 μM) in aqueous acetonitrile, comprised an absorption band centred at ~410 nm (ε = 16900 M^{-1} cm^{-1}), corresponding to the naphthalimide moiety (**Fig. 1a**). Among various metal ions (20 μM), addition of only Fe^{3+} and Cr^{3+} ions induced considerable changes in the absorbance pattern of **1**. Upon addition of Fe^{3+} ions, the absorption intensity of **1** at

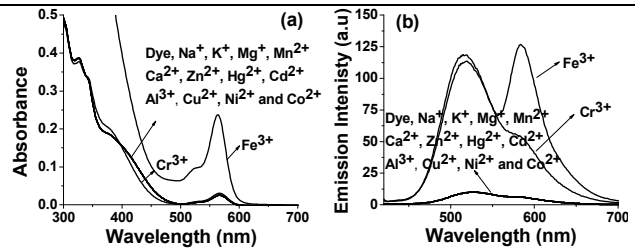

Fig. 1. Metal ion (20 μM) induced variations in the (**a**) absorbance, and (**b**) fluorescence spectra of **1** (10 μM); Excitation wavelength: 400 nm.

~564 nm was enhanced by 10-fold (ε = 24000 M^{-1} cm^{-1}). Whereas, the absorption band centred at ~410 nm was slightly blue shifted by the addition of Cr^{3+} ions The Fe^{3+} induced changes in the absorption pattern of **1** is attributed to Fe^{3+}-induced rhodamine spirolactam ring opening resulting in the formation of **1-Fe^{3+}** complex. The Cr^{3+}-invoked blue shift in the naphthalimide absorption at ~410 nm suggested the formation of **1-Cr^{3+}** complex and indicated the involvement of the piperazine 'N' attached to the naphthalimide moiety of **1** in complex formation. The invariability in the absorption of rhodamine moiety at ~564 nm to the addition of Cr^{3+} denoted the non-involvement of rhodamine moiety in **1-Cr^{3+}** complex formation (**Fig. 1a**).

The dyad probe **1** (10 μM) in aqueous acetonitrile was non-fluorescent owing to the spirocyclic form of rhodamine moiety (Φ = 0.019) and PET induced quenching of fluorescence emission from the naphthalimide moiety (Φ = 0.03) by pyridine 'N'.[9] While the fluorescence pattern of **1** was unaffected by the addition of various metal ions (20 μM), addition of Fe^{3+} and Cr^{3+} ions induced distinct changes in the fluorescence profile of **1** as seen in **Fig. 1b**. Clearly, addition of Fe^{3+} to **1** enhanced the fluorescence intensity in both naphthalimide (Φ = 0.36) and rhodamine (Φ = 0.40) regions due to the formation of **1-Fe^{3+}** complex. The observed enhancement in fluorescence intensities is attributed to the quenching of PET from pyridine 'N' to naphthalimide moiety (~517 nm) and Fe^{3+} induced spirolactam ring opening (~583 nm), which perceptibly indicated the involvement of the pyridine 'N' and rhodamine carbonyl 'O' of **1** in the proposed **1-Fe^{3+}** complex.

Interestingly, the addition of Cr^{3+} (20 μM) to **1** enhanced the fluorescence emission only in naphthalimide region (Φ = 0.33) and not in the rhodamine region (**Fig. 1b**). This patently different fluorescence pattern revealed the involvement of the pyridine 'N' and but not the carbonyl 'O' of rhodamine moiety in **1-Cr^{3+}** complex formation. Thus, the data presented in **Fig. 1** show the apparent difference in the choice of donor atoms selected by the trivalent ions Fe^{3+} and Cr^{3+} during complex formation with the dyad probe **1**. It is imperative to note that Al^{3+}, a possible interfering trivalent ion, did not induce any significant changes in the absorption and fluorescence profiles of **1**.

The difference in the binding environments of Cr^{3+} and Fe^{3+} was further confirmed by NMR analysis. The resonance positions of only the piperazine protons and 'CH_2' protons attached to piperazine 'N' were shifted significantly upon addition of serial concentrations of Cr^{3+} (Fig. S4, ESI†). The observed downfield shift could arise from the possible interactions between Cr^{3+} and the 'N' atoms of piperazine and pyridyl moieties in **1-Cr^{3+}** complex. This proposition was confirmed from the ^{13}C spectrum of **1-Cr^{3+}** complex (Fig. S5, ESI†). Addition of Cr^{3+} resulted in a reduction in intensities of ^{13}C resonances at ~52.4, ~64.3 (corresponding to '$\underline{C}H_2$' units attached to piperazine 'N' atoms) and ~155.5 ppm (attributable to the quaternary carbon of pyridine ring linked to piperazine 'N' *via* CH_2 moiety). It is imperative to note that none of the carbonyl moieties is sensitive to Cr^{3+} ions. The impassive nature of rhodamine carbonyl 'C' at ~165.1 ppm and spirolactam 'C' at ~66.4 ppm to the addition of Cr^{3+} confirmed the non-involvement of rhodamine moiety in **1-Cr^{3+}** complex (Fig. S5, ESI†). On the other hand, a general broadening the ^1H NMR signals of the probe, was observed when Fe^{3+} was added to **1** owing to the strong paramagnetic affect of Fe^{3+}. Similarly, an overall reduction in the intensities of the carbon signals in the ^{13}C NMR spectrum of **1** was observed with the addition of Fe^{3+}. However, the decrement in ^{13}C intensities was much pronounced in the cases of ^{13}C resonances arising from rhodamine carbonyl, spirolactam, piperazine, quinoline and pyridine moieties (Fig. S6, ESI†). This observation corroborated the Fe^{3+} specific UV-visible and fluorescence profiles of **1**, and confirmed the involvement of rhodamine, quinoline and pyridine moieties in **1-Fe^{3+}** complex formation (**Fig. 1**).

The dyad probe **1** (10 μM) was titrated against serial concentrations of Fe^{3+} and Cr^{3+} ions. Successive addition of serial concentrations of Fe^{3+} (0-20 μM) increased the absorption of rhodamine moiety at ~564 nm, progressively and the maximum absorption was observed with 20 μM of Fe^{3+} (**Fig. 2a**). A similar titration with Fe^{3+} ions gradually increased the fluorescence emission from both naphthalimide and rhodamine moieties (**Fig.2b**). The stoichiometry and binding constant of **1-Fe^{3+}** complex ware calculated using fluorescence data (Fig. S7, ESI†) and results indicated the 1:1 stoichiometry of the **1-Fe^{3+}** complex

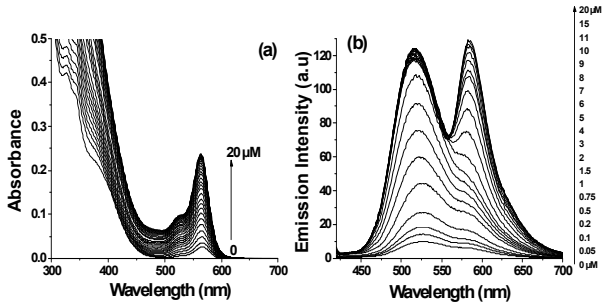

Fig. 2. The Fe^{3+} (0-20 μM) concentration dependent variations in the absorbance (**a**) and fluorescence (**b**) spectra of **1** (10 μM). Excitation wavelength was 400 nm.

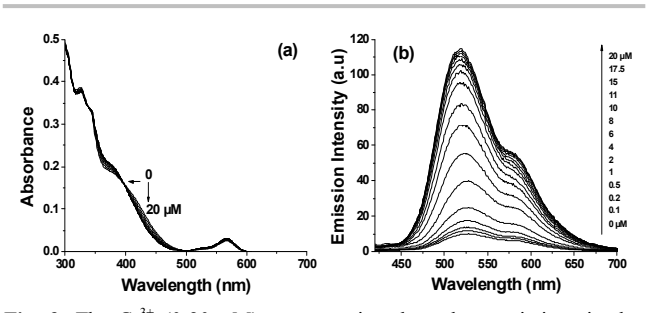

Fig. 3. The Cr^{3+} (0-20 μM) concentration dependent variations in the absorbance (**a**) and fluorescence (**b**) spectra of **1** (10 μM). Excitation wavelength: 400 nm.

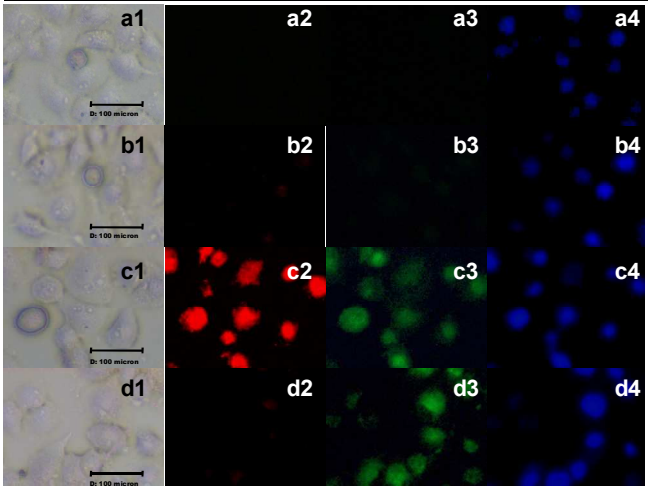

Fig. 4a. Fluorescence microscopic images of A549 cells: Row 1 (**a1-a3**): untreated A549 cells, Row 2 (**b1-b3**): A549 cells treated with **1** (20 μM) alone; Row 3 (**c1-c3**): cells treated with **1** (20 μM) and Fe^{3+} (50 μM); Row 4 (**d1-d3**): cells treated with **1** (20 μM) and Cr^{3+} (50 μM). Column 1 (**a1–d1**), bright field images; Column 2 (**a2–d2**), fluorescence images obtained using red filter; Column 3 (**a3-d3**), fluorescence images obtained using green filter; and Column 4 (**a4–d4**), fluorescence images of Hoechst 33258 dye stained A549 cells.

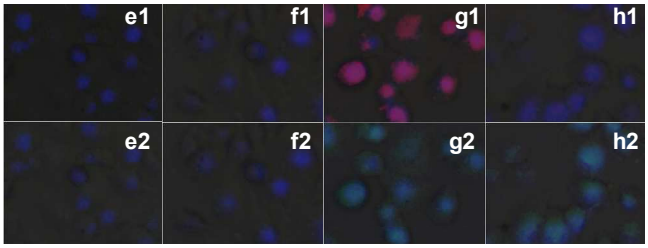

Fig. 4b. Overlaid fluorescence microscopic images of A549 cells: (**e1**) overlaid images of **a1**, **a2** and **a4**; (**f1**) overlaid images of **b1**, **b2** and **b4**; (**g1**) overlaid images of **c1**, **c2** and **c4**; (**h1**) overlaid images of **d1**, **d2** and **d4**; (**e2**) overlaid images of **a1**, **a3** and **a4**; (**f2**) overlaid images of **b1**, **b3** and **b4**; (**g2**) overlaid images of **c1**, **c3** and **c4**; (**h2**) overlaid images of **d1**, **d3** and **d4** of **Fig. 4a**.

with binding constant of 2.2×10^5 M^{-1}.[10] The observed lower detection limit of **1** for Fe^{3+} ions was 1×10^{-8} M (0.6 ppb). Addition of serial concentrations Cr^{3+} (0-20 μM) to **1** (10 μM) gradually shifted the absorption band at ~410 nm corresponding to naphthalimide moiety towards shorter wavelengths as shown in **Fig. 3a**. Under identical conditions the fluorescence emission of **1** increased gradually only from the naphthalimide moiety as shown in **Fig. 3b**. The increment in the fluorescence intensity was linear ($R^2 = 0.993$) in the range from 1×10^{-7} to 1×10^{-5} M and indicated the 1:1 stoichiometry of **1**-Cr^{3+} complex with binding constant as 8.1×10^4 M^{-1} (Fig. S8, ESI†). The lower detection limit of **1** in the case of Cr^{3+} was calculated to be 2×10^{-7} M (10.8 ppb). The detection limits observed for Fe^{3+} / Cr^{3+} using probe **1** are lower than those reported recently for Fe^{3+} / Cr^{3+} using other chemosensors (Table S1, ESI†). Moreover, probe **1** is the first of its kind that is useful for detecting and differentiating Fe^{3+} and Cr^{3+} ions.

Selective detection of Fe^{3+} and Cr^{3+} ions by **1** in the presence of other commonly existing metal ions was studied to assess non-interference of other metal ions. Results from the metal ion competition experiments (Fig. S9, ESI†), confirmed the Fe^{3+} and Cr^{3+} detection ability of **1** even in the presence of other commonly coexisting metal ions using the signature absorption and fluoresce profiles generated (**Figs. 1-3**) upon interaction with Fe^{3+} or Cr^{3+}. As the intracellular concentrations of Fe^{3+} and Cr^{3+} are at micromolar levels, the detection of Fe^{3+} / Cr^{3+} at ppb levels in the present study demonstrated the probe's eligibility for the detection of intracellular Fe^{3+} / Cr^{3+} ions.[11] Stability at physiological pH and low cytotoxicity are the key criteria for living cell imaging, the effect of pH on the fluorescence emission pattern of **1** was evaluated. Results illustrated the stability of **1** in the range of pH 6-10 (Fig. S10, ESI†) and revealed its suitability to operate at physiological pH. Moreover, the results of MTT assay (Fig. S11, ESI†) showed that after 48 h of cellular internalization of **1** (20 μM), both cancerous (A549) and endothelial (ECV-304) cells remained viable (more than 95%), indicated the biocompatibility of **1** to cells under experimental conditions.

We next explored the utility of **1** in sensing the presence of Fe^{3+} and Cr^{3+} ions in biological systems. The cancerous A549 and non-cancerous CHO cells were used for *in vitro* experiments (**Fig. 4a** and Fig. S13, ESI†). The untreated A549 cells (**a1-a4**) and cells treated with **1** (20 μM) alone (**b1-b4**) were non-fluorescent. However, the A549 cells pre-incubated with **1** (20 μM) triggered bright red (**c2**) and green fluorescence (**c3**) upon treatment with Fe^{3+} (50 μM) ions. Under similar conditions, A549 cells pre-treated with **1** (20 μM) exhibited bright green (**d3**) but not red (**d2**) fluorescence upon incubating with Cr^{3+} (50 μM) ions. In all groups, nuclear staining was done with Hoechst 33258 dye (**a4**, **b4**, **c4** and **d4**). Additionally, A549 cells treated with only Fe^{3+} (50 μM) or Cr^{3+} (50 μM) did not show any fluorescence (Fig. S15, ESI†). The overlaid fluorescence microscopic images provided in **Fig. 4b** indicate, clearly, the potential of probe **1** to get into the cytoplasmic compartments as well as the nucleus of A549 cells. Similar bio-imaging properties were observed even for non-cancerous CHO cells (Fig. S13 and S17, ESI†). Thus, the data shown in **Fig. 4** and Figs. S12-S18, ESI†, clearly demonstrated the Fe^{3+} and Cr^{3+} ion specific detection ability of dyad probe **1** in live cells.

In conclusion, we have reported a rhodamine-naphthalimide dyad probe **1** for the selective detection of Fe^{3+} or Cr^{3+} ions present in aqueous and biological systems. The multiple metal coordination sites available in the single molecular probe **1** offer distinct chelation environments for Fe^{3+} and Cr^{3+} ions, and thereby emit metal ion specific fluorescence at two different wavelengths. The presence of other competitive metal ions, including Al^{3+}, does not affect the sensing ability of **1**. Probe **1** is the first of its kind, and can be used for sensing intracellular Fe^{3+} and Cr^{3+} ions in a single assay.

Acknowledgments

N. R. Ch. thanks the CSIR, India, for CSIR-Nehru Science Postdoctoral Fellowship. AKB thanks UGC, India, for a Senior Research Fellowship. CRP thanks to DST, India for 'Ramanujan Fellowship Grant' (SR/S2/RJN-04/2010; GAP0305). Financial support from CSIR 12th plan projects CSC0201 and CSC0302 is acknowledged. Financial support from 'INTELCOAT' project is also acknowledged.

Notes and references

[a]*Organic Chemistry Division, CSIR-Central Leather Research Institute, Adyar, Chennai-600 020, India.*
[b]*Crop Protection Chemicals, cBiomaterials Group, CSIR-Indian Institute of Chemical Technology, Tarnaka, Hyderabad-500 007, India.*
chereddynarendra@gmail.com; thennarasu@gmail.com

† Electronic Supplementary Information (ESI) available: Experimental procedures, NMR, ESI-MS spectra, metal ion competitive expreriments, effect of pH, cell viability assay and live cell imaging experiments. See DOI: 10.1039/b000000x/

1 (a) P. Aisen, M. Wessling-Resnick and E. A. Leibold, *Curr. Opin. Chem. Biol.*, 1999, **3**, 200; (b) R. S. Eisenstein, *Annu. Rev. Nutr.*, 2000, **20**, 627; (c) T. A. Rouault, *Nat. Chem. Biol.*, 2006, **2**, 406.

2 (a) A. K. Singh, V. K. Gupta and B. Gupta, *Anal. Chim. Acta,* 2007, **585**, 171; (b) J. B. Vincent, *Proc. Nutr. Soc.*, 2004, **63**, 41. (c) R. A. Anderson, *Regul. Toxicol. Pharmacol*., 1997, **26**, S35. (d) W. Mertz, *J. Nutr.* 1993, **123**, 626.

3 (a) C. Brugnara, *Clin. Chem*., 2003, **49**, 1573; (b) N. C. N. Andrews, *Engl. J. Med*., 1999, **341**, 1986.

4 (a) S. Fakih, M. Podinovskaia, X. Kong, H. L. Collins, U. E. Schaible and R. C. Hider, *J. Med. Chem*., 2008, **51**, 4539; (b) X. Wu, B. Xu, H. Tong and L. Wang, *Macromolecules*, 2010, **43**, 8917; (c) S. Smanmoo, W. Nasomphan and P. Tangboriboonrat, *Inorg. Chem. Commun*., 2011, **14**, 351; (d) N. Bian, Q. Chen, X.-L. Qiu, A.-D. Qi and B.-H. Han, *New J. Chem*., 2011, **35**, 1667.

5 (a) H. M. Wu, P. Zhou, J. Wang, L. Zhao and C. Y. Duan, *New J. Chem*., 2009, **33**, 653; (b) M. Sarkar, S. Banthia and A. Samanta, *Tetrahedron Lett.*, 2006, **47**, 7575; (c) S. Guha, S. Lohar, A. Banerjee, I. Hauli and D. Das, *Talanta,* 2012, **91**, 18.

6 (a) B. Wang, J. Hai, Z. Liu, Q. Wang, Z. Yang and S. Sun, *Angew. Chem. Int. Ed*., 2010, **49**, 4576; (b) Jy D. Chartres, M. Busby, M. J. Riley, J. J. Davis and P. V. Bernhardt, *Inorg. Chem*., 2011, **50**, 9178; (c) N. R. Chereddy, S. Thennarasu and A. B. Mandal, *Dalton. Trans.,* 2012, **41**, 11753; (d) N. R. Chereddy, S. Thennarasu and A. B. Mandal, *Analyst,* 2013, **138**, 1334; (e) N. R. Chereddy, K. Suman, P. S. Korrapati, S. Thennarasu and A. B. Mandal, *Dyes Pigm.*, 2012, **95**, 606; (f) A. J. Weerasinghe, C. Schmiesing, S. Varaganti, G. Ramakrishna and E. Sinn, *J. Phys. Chem. B*, 2010, **114**, 9413.

7 P. Mahato, S. Saha, E. Suresh, R. D. Liddo, P. P. Parnigotto, M. T. Conconi, M. K. Kesharwani, B. Ganguly and A. Das, Inorg. Chem., 2012, **51**, 1769; (b) K. W. Huang, H. Yang, Z. G. Zhou, M. X. Yu, F. Y. Li, X. Gao, T. Yi and C. H. Huang, *Org. Lett*., 2008, **10**, 2557; (c) Z. G. Zhou, M. X. Yu, H. Yang, K. W Huang, F. Y Li, T. Yi and C. H. Huang, *Chem. Commun*., 2008, **29**, 3387.

8 (a) A. Barba-Bon, A. M. Costero, S. Gil, M. Parra, J. Soto, R. Martınez-Manez and F. Sancenon, *Chem. Commun*., 2012, **48**, 3000; (b) X. Chen, X. Y. Shen, E. Guan, Y. Liu, A. Qin, J. Z. Sun and B. Z. Tang, *Chem. Commun*., 2013, **49**, 1503; (c) S. Goswami, K. Aich, S. Das, A. K. Das, D. Sarkar, S. Panja, T. K. Mondal and S. Mukhopadhyay, *Chem. Commun*., DOI: 10.1039/c3cc46860g; (d) J. Mao, L. Wang, W. Dou, X. Tang, Y. Yan and W. Liu, *Org. Lett*., 2007, **9**, 4567.

9 L. Xu, Y. Xu, W. Zhu, C. Yang, L. Han and X. Qian, *Dalton Trans*., 2012, **41**, 7212.

10 J. Hatai, S. Pal, G. P. Jose, T. Sengupta and S. Bandyopadhyay, *RSC Adv*., 2012, **2**, 7033.

11 (a) E. Mills, X.-P. Dong, F. Wang and H. Xu, *Future Med. Chem*., 2010, **2**, 51; (b) A. Pechova and L. Pavlata, *Vet. Med*. 2007, **52**, 1.